

## Geoid-Determination in the Norwegian-Greenland Sea – An Assessment of Recent Results

C. C. Tscherning/René Forsberg

Geodetic Institute, Gamlehavn Allé 22, DK-2920 Charlottenlund, Denmark

### Key Words

Spherical harmonic expansion  
Geoid undulations  
Norwegian-Greenland Sea

### Abstract

The Goddard Earth Model 10C and a model based upon Rapp's potential coefficient solution complete to degree and order 180 are compared with Doppler-derived geoid undulations, SEASAT-A altimeter values and point free-air gravity anomalies in the Norwegian-Greenland Sea and in the coastal areas. An agreement between observed and computed geoid undulations is found at the 1–2 m level, between observed and computed gravity anomalies at the 27 mgals level (compared to a r.m.s.v. of the observed values of  $\pm 46$  mgal). A comparable result is found for deflections of the vertical in the Scandinavian area. It is pointed out, that collocation is a suitable method for making local corrections to or improvements of a global gravity field model. This is illustrated through the computation of an improved geoid for the area bounded by  $66.5^\circ < \varphi < 69.5^\circ$ , and  $7.5^\circ < \lambda < 16.5^\circ$ . Finally the calculated geoid based on Rapp's coefficients is compared with undulations derived solely from the isostatically compensated sea-bottom topography. This comparison exposes geophysical information, which otherwise is not clearly seen.

### 1. Introduction

Let us define the geoid as the equipotential surface of the Earth's gravitational potential ( $W$ ), which most closely approximates mean sea level. We will regard  $W$  as being constant in time, i.e. all changes due to atmospheric variations, changes in the Earth's movement in space, the tidal variations etc. are removed. Let us also suppose, that we have adopted a normal or reference potential,  $U$ , e.g. consistent with the parameters of the Geodetic Reference System 1980, (GRS 1980), (see Moritz, 1980). In  $U$  we also include the potential of all masses external to the surface of the Earth. The anomalous potential,  $T = W - U$ , will then be a harmonic function in space.

The geoid height ( $N$ ) above the reference ellipsoid can then be computed to a good approximation using Brun's formula,

$$N = T/\gamma, \quad (1)$$

where  $\gamma = |\nabla U|$ , the normal gravity. (Note, that in modern geodesy, the geoid height,  $N$ , has been substituted by the height anomalies,  $\zeta$ , which is the height above the "telluroid". Brun's formula (1) is still valid, now with  $N$  replaced by  $\zeta$ ).

A number of techniques are available for the determination of  $T$  and thereby for the determination of  $N$  (or  $\zeta$ ): Stokes integral formula, least-squares collocation, least squares or least norm approximation, see Heiskanen and Moritz (1976), Tscherning (1978, 1981).

Recently, it has been possible to obtain "direct" measurements of  $N$ . One type is the so-called doppler determined geoid undulations. Using doppler satellite techniques, the Cartesian coordinates ( $X, Y, Z$ ) of a point may be determined. This permits the computation of the height,  $h$ , above the reference ellipsoid. If the height above mean sea level (the orthometric height)  $H$ , is known we have

$$N \approx \zeta \approx h - H \quad (2)$$

(In points at the mean sea surface, we have  $N = \zeta = h$ ).

Altimeter data collected by the satellites Geos-3 and SEASAT-A may also be used for the determination of the geoid at sea. This is done through the use of an elaborated adjustment procedure, see e.g. Lerch et al. (1981), Rapp (1978, 1979). Through this procedure, the main part of the time-varying disturbances of the sea-surface (tides, waves, etc.) are removed and a quasi-stationary sea-surface topography is determined. If we neglect the difference between this surface and the geoid (estimated to be below 1 m), then the geoid is determined. Doing this Geos-3 and SEASAT-A altimeter data have been used to determine the geoid in ocean areas up to latitudes  $63^\circ$  and  $72^\circ$ , respectively.

Before the occurrence of these possibilities for direct geoid determination, the main source of our gravity field knowledge was the free-air gravity anomalies,  $\Delta g$ . They are related to  $T$  through the following equation (in spherical approximation),

$$\Delta g = -\frac{\partial T}{\partial r} - \frac{2}{r} \cdot T, \quad (3)$$

where  $r$  is the distance of the point of evaluation from the origin.

The (point) values are used for the computation of mean free air gravity anomalies,  $\bar{\Delta g}$ , of blocks of various sizes, such as  $5^\circ \times 5^\circ$  or  $1^\circ \times 1^\circ$ . These mean values are important in geoid determinations, when e.g. Stokes integral formula

is used. In many areas both on land and at sea these quantities are, however, poorly determined, simply due to the lack of point values.

This situation has changed dramatically at sea, because the altimeter determined geoid undulations have been used for the computation of mean gravity anomalies, see (Rapp, 1978).

Long-wavelength gravity field information is also obtained through the analysis of satellite orbit perturbations. This information has then in combination with  $5^\circ \times 5^\circ$  or  $1^\circ \times 1^\circ$  mean gravity anomalies been used for the determination of approximation,  $\tilde{W}$ , to  $W$ , and thereby for the determination of  $N$ . (See e.g. Rapp (1977, 1978, 1979), Lerch et al. (1979), Lerch et al. (1981), Reigber et al. (1980).

The results are given as sets of "potential coefficients"  $\tilde{C}_{ij}, \tilde{S}_{ij}, 0 \leq j \leq i, 0 \leq i \leq n$ , so that

$$\begin{aligned} \tilde{W}(r, \theta, \lambda) = & \frac{GM}{r} \sum_{i=0}^n \left(\frac{a}{r}\right)^i \bar{P}_{ij}(\cos\theta) \cos(j\lambda) \tilde{C}_{ij} \\ & + \sin(j\lambda) \tilde{S}_{ij} + \frac{\omega^2}{2} (X^2 + Y^2) \end{aligned} \quad (4)$$

Here  $\theta$  is the (geocentric) co-latitude,  $\lambda$  the longitude,  $GM$  the product of the gravitational constant and the mass of the Earth,  $a$  the semi-major axis of the reference ellipsoid,  $\bar{P}_{ij}$  the fully normalized associated Legendre polynomials and  $\omega$  the angular velocity of the Earth. Some of the solutions are given names such as GEM 10 C (= Goddard Earth Model no. 10C). We will also name Rapp's recent solution, complete up to and inclusive  $n = 180$ , by "Rapp-180".

The purpose of this paper is not to discuss or explain different methods for geoid determination, but to investigate the results obtained in a specific area, the Norwegian-Greenland Sea, (defined here as the ocean area bounded by  $60^\circ < \varphi < 80^\circ, -25^\circ < \lambda < 20^\circ$ ), and the possibilities we have for making simple improvements of or corrections to the obtained results.

The most detailed solutions are Rapp-180 and GEM 10C, which both include coefficients up to and inclusive degree 180. These solutions have therefore in the following been used as the basis for all investigations.

In section 2 we explain briefly the procedures used for evaluating  $N$  and related quantities such as deflections of the vertical and gravity anomalies. In section 3 we give results of comparisons with doppler derived geoid undulations, point free-air gravity anomalies, SEASAT-A geoid undulations and deflections of the vertical. Possible local improvements are discussed in section 4, and a local improvement for a  $3^\circ \times 9^\circ$  area in the Norwegian Sea is presented.

Finally in section 5 the influence of the bathymetry and the isostatic compensation in the Norwegian-Greenland Sea is investigated, along with a short discussion of the application of geoid undulations in geophysical investigations.

## 2. Evaluation of Series of Spherical Harmonics of High Degree

A simple algorithm for the computation of 0, 1, and 2 order derivatives of a series in spherical harmonics is given in

(Tscherning, 1976). This algorithm broke down using 10 1/2 digit arithmetic at degree 90. A modified version of Clenshaw's algorithm was then designed based on ideas described in Gerstl (1978). (The modified algorithm permits the computation of the derivatives of the series). The results of the algorithm agrees well with results obtained using an algorithm developed by O. Colombo and C. Rizos (Rizos, 1979). Using the coefficients Rapp-180 and GEM 10C with  $GM, a, \omega,$  and  $U$  equal to the GRS 1980 values, we then computed geoid undulations in the Greenland-Norwegian Sea. Eq. (1) was used with  $T = \tilde{W} - U$ , see Fig. 1A and 1B.

Gravity anomalies were computed using eq. (3). The values derived from Rapp-180 are shown in Fig. 2.

A slightly more stringent procedure was used for the deflections of the vertical. Using the components of the gradient of  $\tilde{W}$ , we first computed approximate values of the astronomical latitude and longitude, cf. Heiskanen and Moritz (1967, eq. (2.29)). The deflections were then computed using *Ibid.* eq. (2-140).

## 3. Assessment of the Rapp-180 and the GEM 10C Coefficient Sets

The Rapp-180 coefficient set has been assessed in two ocean areas, the Tonga Trench and the Indian Ocean, cf. Rapp (1980). The GEM 10C coefficient set has been assessed using 20 Geos-3 arcs cf. (Lerch et al. 1981, Table II). An excellent agreement was found with observed geoid undulations (cf. section 1) and with results obtained from other techniques at the 1 m level. Note, that in both cases, Geos-3 altimeter data in the areas were used in the determination of the coefficients.

In the part of the Norwegian-Greenland Sea north of latitude  $63^\circ$  only mean gravity anomalies were used for the determination of the coefficients. It is hence interesting to compare the geoid undulations determined from SEASAT-A altimeter data with the geoid undulations computed based on the two coefficient sets. Such data were available to us in the form of a map (private communication by S. Klosko, 1980), from which about 250 values were read in the nodes of a grid with a distance of  $1^\circ$  in latitude and  $2^\circ$  in longitude between the nodes. An excellent agreement was found, with a standard deviation of  $\pm 0.9$  m —  $\pm 1.6$  m and a bias of 3 m, see Table I. This bias is caused mainly by the different reference ellipsoids used.

In the area we have doppler-derived geoid undulations available in a number of points at the Greenland east coast, the Faroe Islands, an oil-rig in the Norwegian Sea and in Norway. (The values in Norway and off the Norwegian coast were made available to us by Norges geografiske Oppmåling). The (X, Y, Z) coordinates were given in the NWL9D coordinate system. These values were transformed to a (hopefully) geocentric coordinate system using the following transformation

$$\begin{Bmatrix} X_{new} \\ Y_{new} \\ Z_{new} \end{Bmatrix} = \begin{Bmatrix} \Delta X \\ \Delta Y \\ \Delta Z \end{Bmatrix} + (1 + \Delta L) \begin{Bmatrix} 1 & -\epsilon_3 & \epsilon_2 \\ \epsilon_3 & 1 & -\epsilon_1 \\ -\epsilon_2 & \epsilon_1 & 1 \end{Bmatrix} \begin{Bmatrix} X_{old} \\ Y_{old} \\ Z_{old} \end{Bmatrix} \quad (5)$$

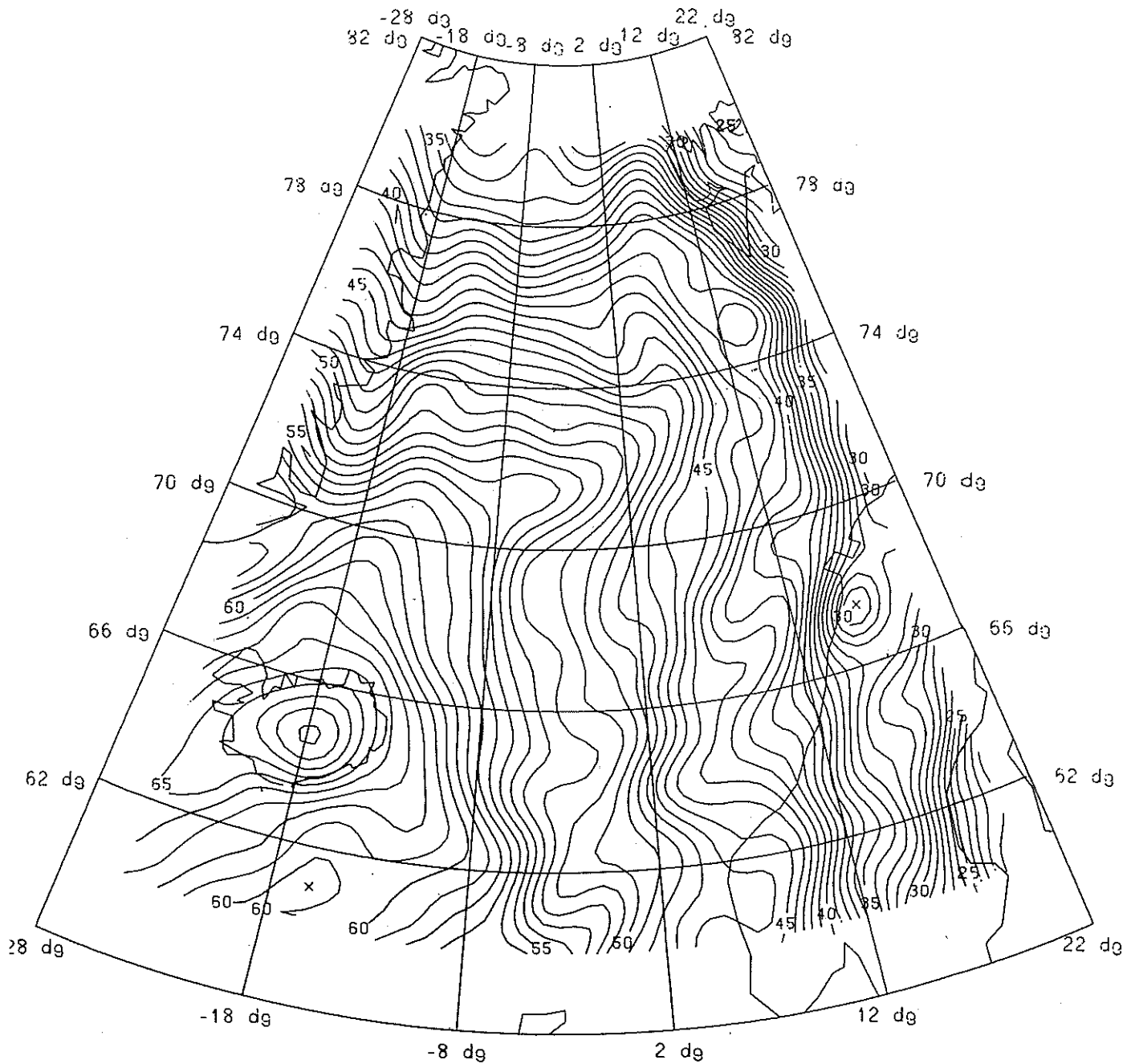


Fig. 1A  
GRS 1980-geoid calculated using Rapp-180. Contour interval 1 m.

with  $\Delta X = \Delta Y = 0$ ,  $\Delta Z = +4$  m (Grappo (1980)),  $\Delta L = -0.4 \times 10^{-6}$ ,  $\epsilon_1 = \epsilon_2 = 0$  and  $\epsilon_3 = -0.8$ . The results agree with a standard deviation of  $\pm 1$  m, however a bias of  $-2$  m and  $4$  m was found for the East-Greenland and the Faroe Island stations, respectively, see Table I.

Using eq. (3) we computed free-air anomalies in 289 points in the area bounded by latitude  $66^\circ$  south, and  $70^\circ$  north,

and by longitude  $6^\circ$  west and  $18^\circ$  east, see Fig. 8. The result of the comparison is given in Table I.

Finally, the deflections of the vertical in about 300 stations in Scandinavia were computed as described in section 2. The values were transformed to ED1950 using the datum shift given in Ordnance Survey (1981) modified as recommended in Grappo (1980). The observed values and the

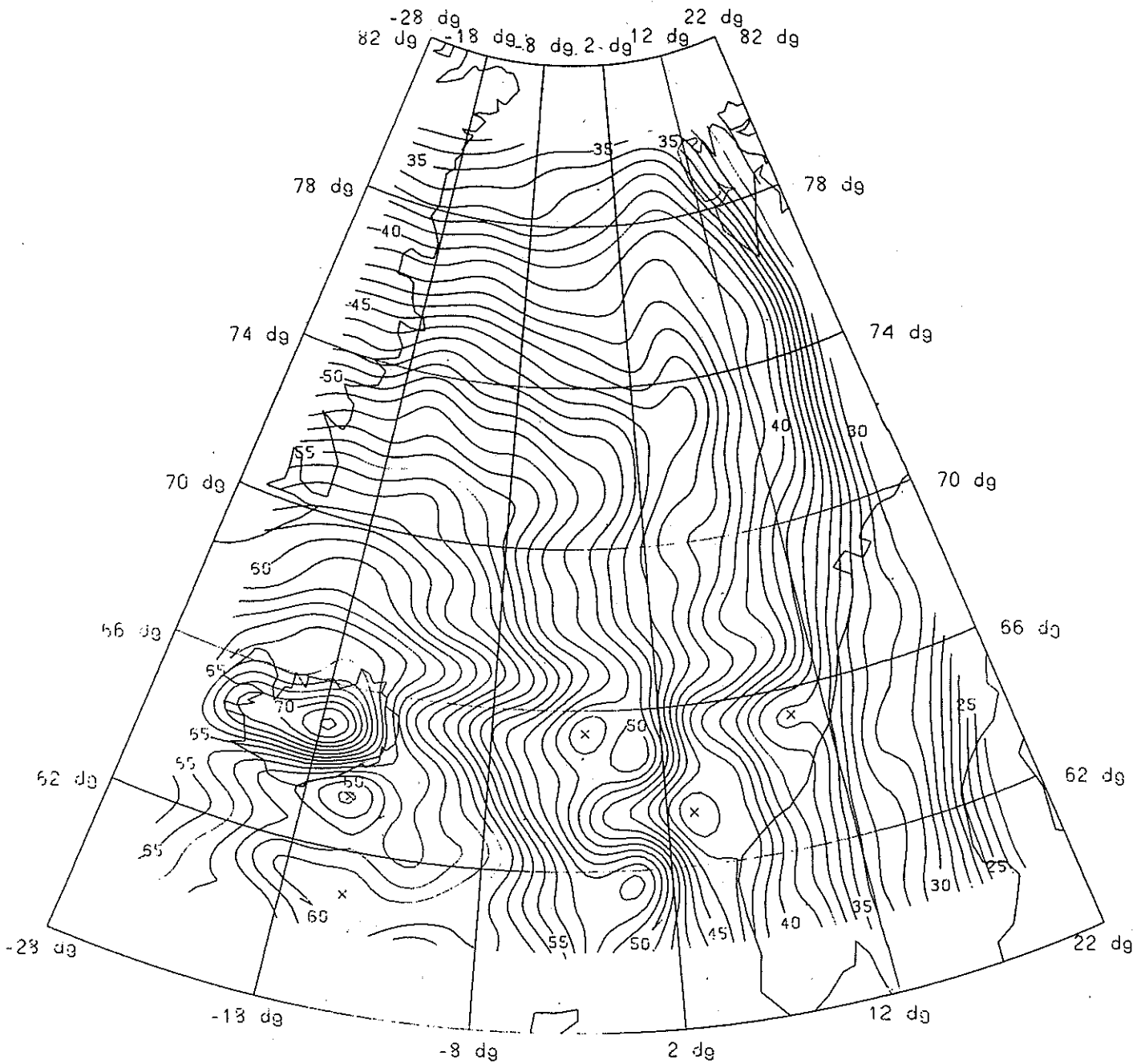


**Fig. 1B**  
GRS 1980-geoid calculated using GEM10C. Contour 1 m.

differences between observed and values computed based on Rapp-180 are shown in Fig. 3, 4, respectively. The result of the comparison expressed in terms of mean and standard deviation is given in Table I for both sets of coefficients. It seems that the Rapp-180 coefficient set is superior to the GEM 10C coefficient set in the Norwegian-Greenland sea and in the coastal areas.

In any case, the results are under all circumstances excellent, and show that the coefficients contain a tremendous amount of information. However, if the coefficients had been error-free, we should have got an even better agreement. The variation of geoid undulations referring to an errorfree 180-degree field may be estimated based on the e.g. the degree-variance model developed in Tscherning and Rapp (1974). Let us denote this variation by  $\sigma_{180}^2(\xi)$ .

**Table I:** Comparison between observed values and values computed based on GEM 10C, the Rapp-180 coefficient set or on a locally improved solution.  
 $\bar{x}$  = mean value,  $\sigma$  = standard deviation.

Observation	Number of values	Observed	Difference Observed — computed from		Difference observed — computed based on local data
			GEM 10C	Rapp-180	
Free-air gravity within $66^\circ < \varphi < 75^\circ$ $6^\circ < \lambda < 18^\circ$	289	$\bar{x}$ — 0.1 mgal $\sigma$ $\pm$ 46.0 mgal	— 10.1 $\pm$ 41.3	— 7.4 mgal $\pm$ 26.1 mgal	(Due to the use of collocat.) 0.0 mgal $\pm$ 2.0 mgal
$\zeta$ Deflections of the vertical in Scandinavia	312	$\bar{x}$ — 2".39 $\sigma$ $\pm$ 3".83	— 1".18 $\pm$ 3".37	— 0".35 $\pm$ 2".72	
	294	$\bar{x}$ 2".97 $\sigma$ $\pm$ 4".66	0".85 $\pm$ 3".83	— 0".17 $\pm$ 3".15	
Doppler derived geoid undulations: DK + N	17	$\bar{x}$ 32.0 m $\sigma$ $\pm$ 4.7 m	1.9 m $\pm$ 2.2 m	0.1 m $\pm$ 1.0 m	— 0.5 m
Station no. 30439	1	— 34.0 m	— 1.8 m	— 1.8 m	
East Greenland	2	$\bar{x}$ 59.2 m $\sigma$ $\pm$ 3.3 m	4.3 m $\pm$ 0.4 m	4.0 m $\pm$ 0.8 m	
Faroe Islands	3	$\bar{x}$ 47.0 m $\sigma$ $\pm$ 0.9 m	— 2.3 m $\pm$ 0.3 m	— 2.5 m $\pm$ 0.4 m	
SEASAT-A geoid undulations, within $60^\circ < \varphi < 69^\circ$ $-25^\circ < \lambda < 14^\circ$	216	$\bar{x}$ not computed $\sigma$ computed	3.0 $\pm$ 1.6	3.5 m $\pm$ 0.9 m	
SEASAT-A geoid undulations, within $67^\circ < \varphi < 69^\circ$ $6^\circ < \lambda < 13^\circ$	15	$\bar{x}$ not computed $\sigma$ computed		2.9 m $\pm$ 1.1	3.1 m $\pm$ 1.0 m

Then

$$\sigma_{180}^2(\zeta) = \sum_{n=181}^{\infty} \sum_{m=0}^n (\bar{C}_{nm}^2 + \bar{S}_{nm}^2) \left(\frac{R_b}{R}\right)^{2n} \cdot R^2,$$

where  $R$  is the mean radius of the Earth,  $R_b$  (= 6369.8 km) is the radius of the Bjerhammar-Sphere and

$$\sum_{m=0}^n (\bar{C}_{nm}^2 + \bar{S}_{nm}^2) R^2 \approx \frac{1.79371 \times 10^4}{(n-2)(n-2)(n+24)} \text{ m}^2$$

Using the subroutine COVA (cf. *Ibid*, appendix) we get

$$\sigma_{180}^2(\zeta) = 0.2 \text{ m}^2$$

Let us put the variance of the difference between observed and computed geoid undulations equal to  $1.0 \text{ m}^2$ , and let us contribute 50% of the error to the coefficients. Then the error due to the error in the coefficients is  $0.4 \text{ m}^2$ . If the error in the coefficients is the same for all coefficients and

if the errors are uncorrelated, then an individual coefficient will have a standard deviation of  $\pm 0.5 \times 10^{-9}$ , which is not an unreasonable estimate.

#### 4. Possibilities for Local Improvements

In Fig. 4 the differences between observed and computed deflections of the vertical were shown. They are generally much smaller than the observed values, cf. Table I. However, the differences are in a few places much larger than the observed values. We know, however, that there are large discrepancies between different sets of mean gravity anomalies, cf. eg. (Wenzel, 1980) which indicate that some of these values must be wrong.

If we find out, that some values used for the determination of a set of potential coefficients are wrong, then it is obviously not possible to update a coefficient set complete to

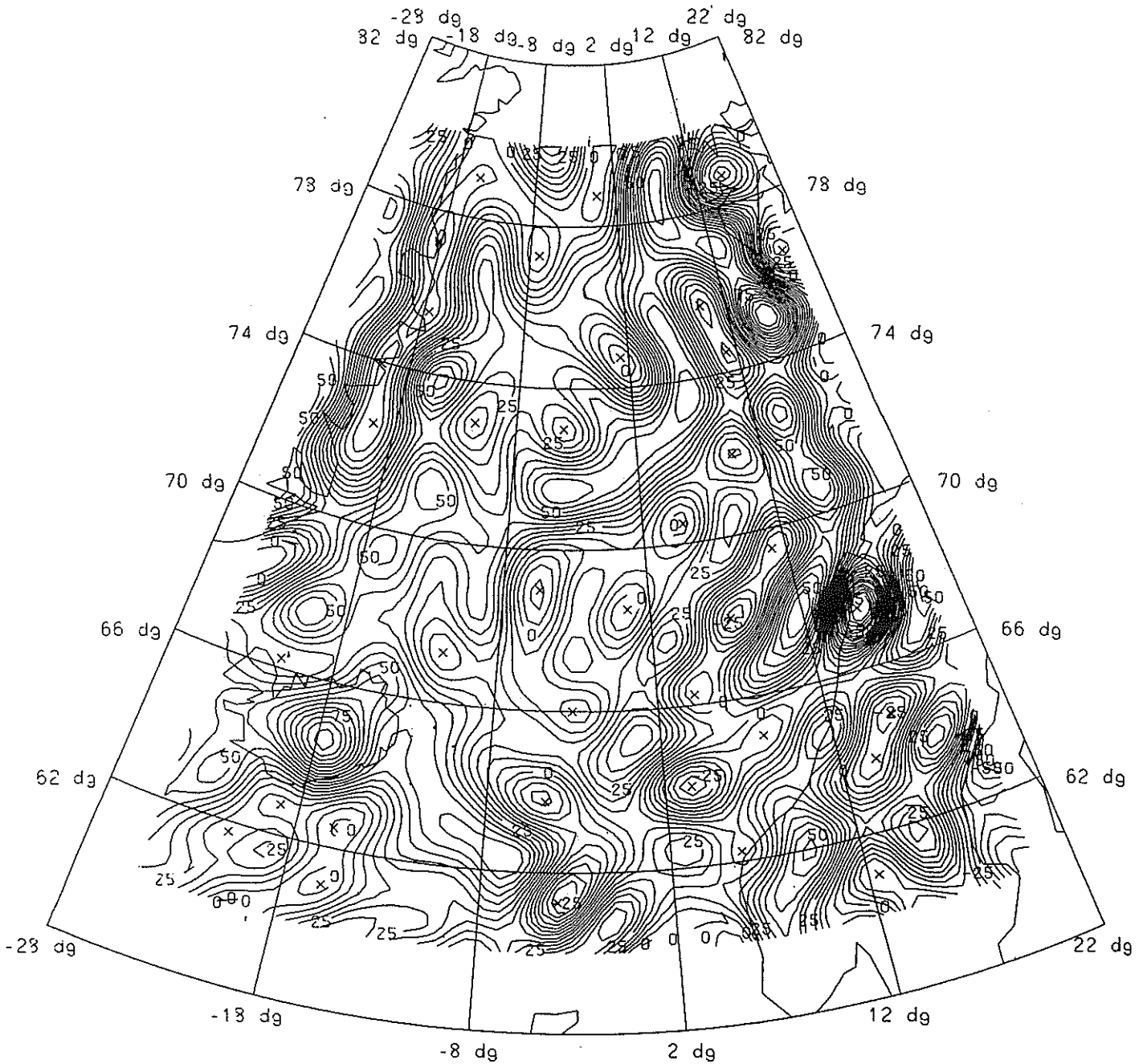


Fig. 2  
Free-air gravity anomalies calculated using Rapp-180. (Reference System GRS 1980). Contour interval 5 mgal.

degree 180. We may, however, use a technique such as least-squares collocation in order to update the approximation to the anomalous potential determined by the coefficients. The residual values with respect to  $\tilde{T}_0 = \tilde{W} - U$  are used to compute an approximation  $\tilde{T}_1$  using collocation, and the corrected solution will then be  $\tilde{T}_0 + \tilde{T}_1$ . (This corresponds to step 1 in stepwise collocation, see Tscherning (1978)). Least-squares collocation will determine a harmonic function ( $\tilde{T}_1$ ), as smooth as possible, which agrees with the ob-

served (residual) values. The smoothness property will make  $\tilde{T}_1$  very small in areas without observations, a property we exactly need in this situation (see Fig. 8). If local data are available (topographic heights, bathymetry, gravity anomalies, deflections of the vertical), then such data may be used for the construction of local improvements to the geoid (or to the gravity potential). Here one may use collocation, Stokes integral formulae or another suitable technique, see e.g. Forsberg and Tscherning (1981),

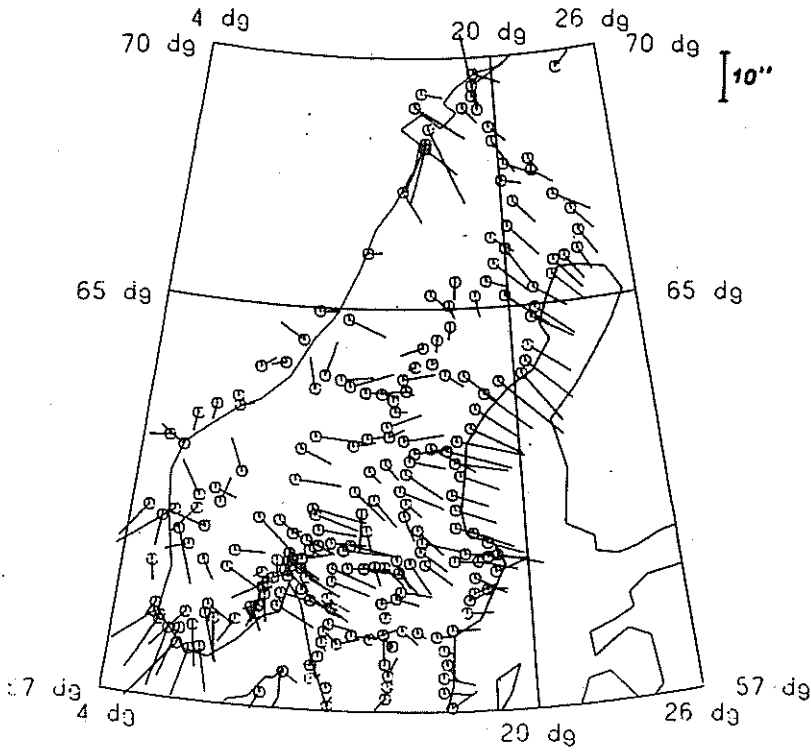


Fig. 3  
Observed deflections of the vertical in ED 1950.

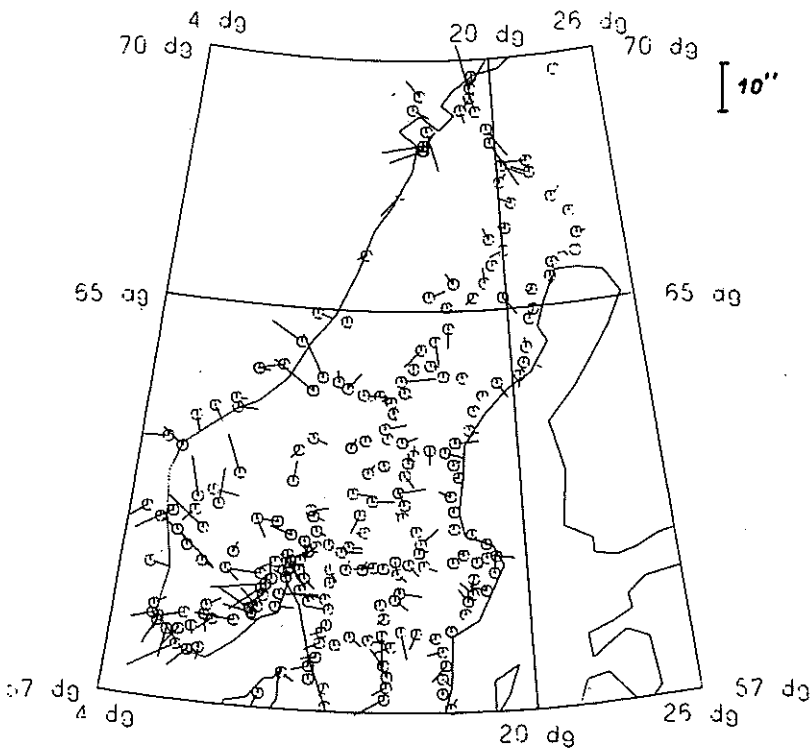
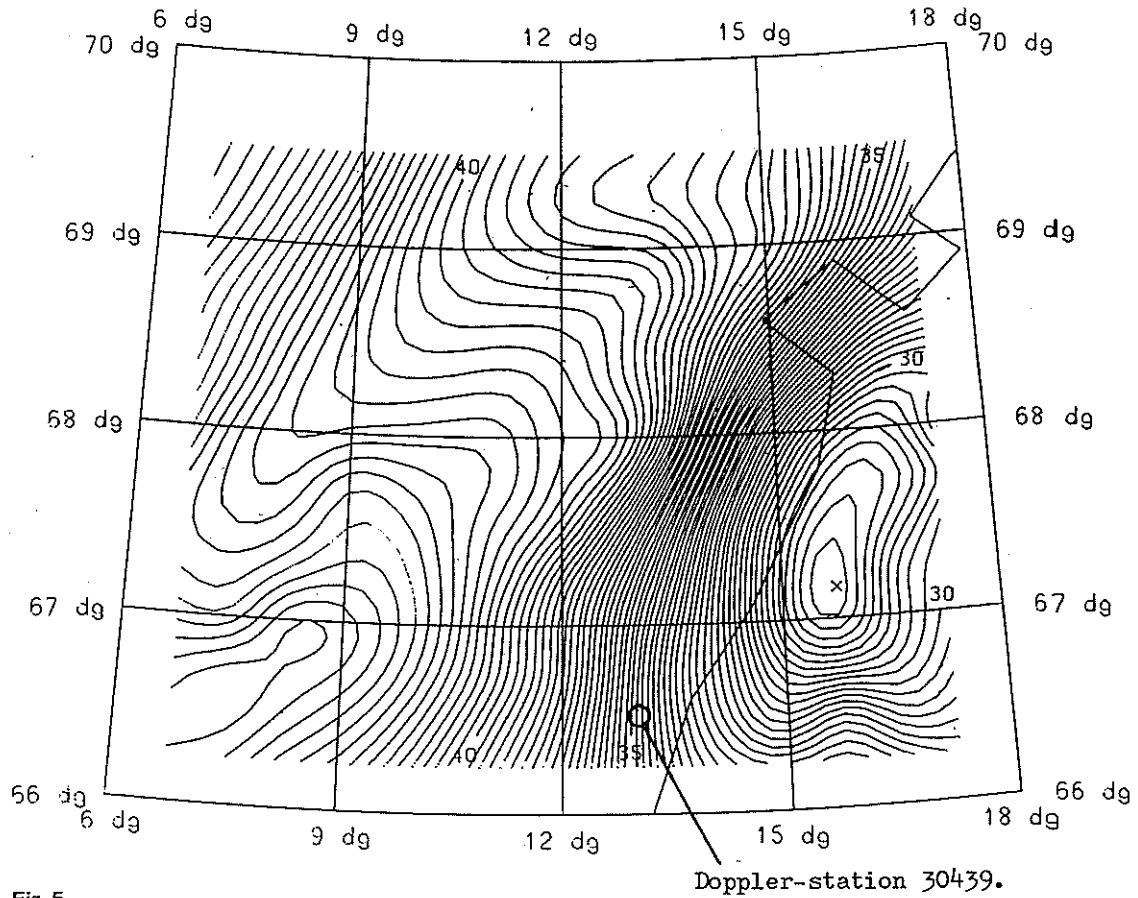
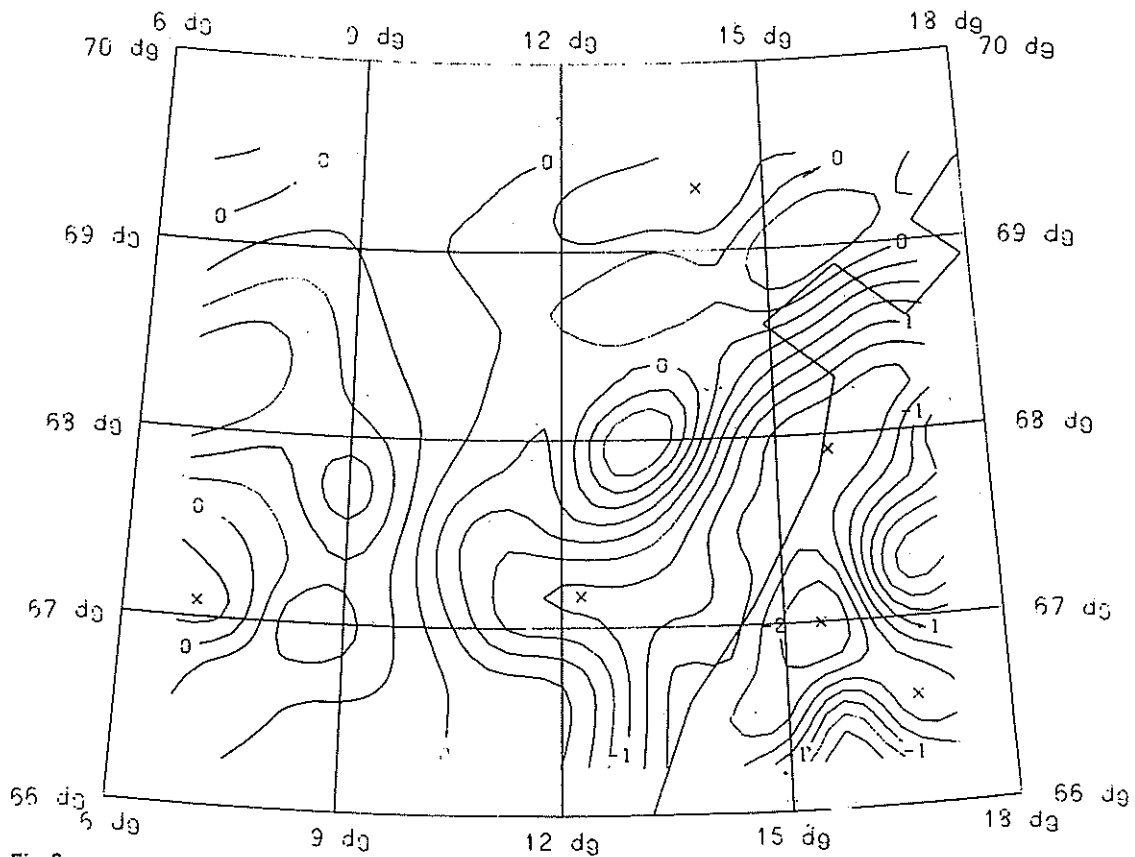


Fig. 4  
Difference between observed deflections and deflections computed using Rapp-180 and transformed to ED 1950.



**Fig. 5**  
 Geoid undulations in an area near the north coast of Norway based on Rapp-180 and local gravity information, computed using collocation. Contour interval 0.25 m.



**Fig. 6**  
 The local improvements to the geoid obtained from the gravity data. Contour interval 0.25 m.



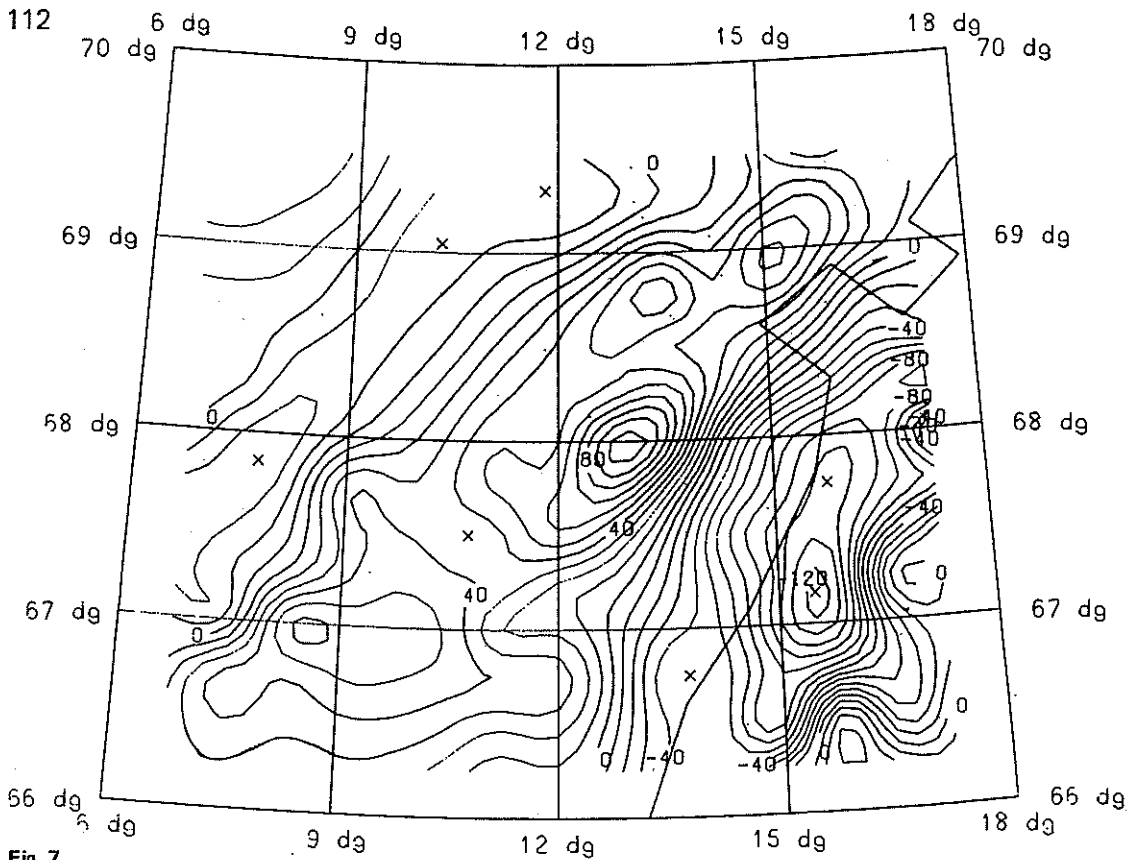


**Fig. 7**  
The local gravity anomaly field interpolated using collocation. Contour interval 10 mgal.

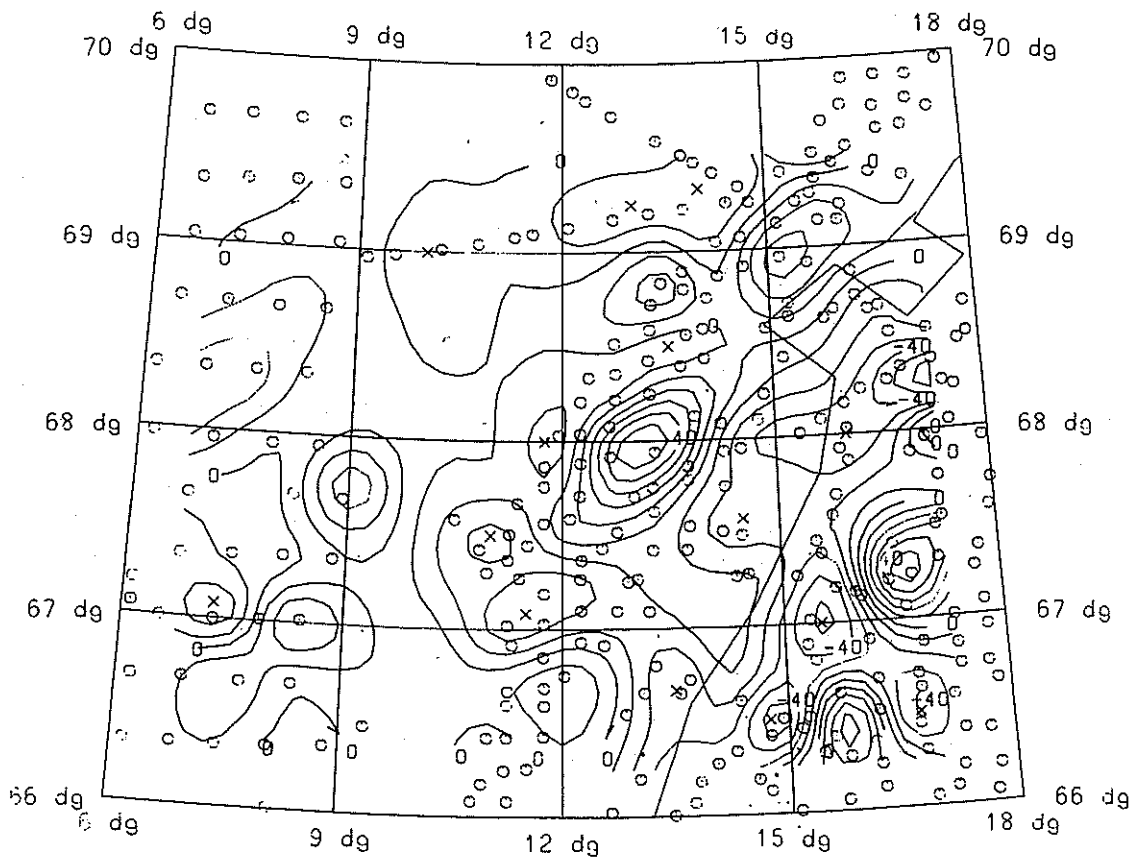


**Fig. 8**  
The difference between the interpolated free-air anomalies and the anomalies computed based on Rapp-180. Contour interval 10 mgal. Position of observed gravity values shown by o.

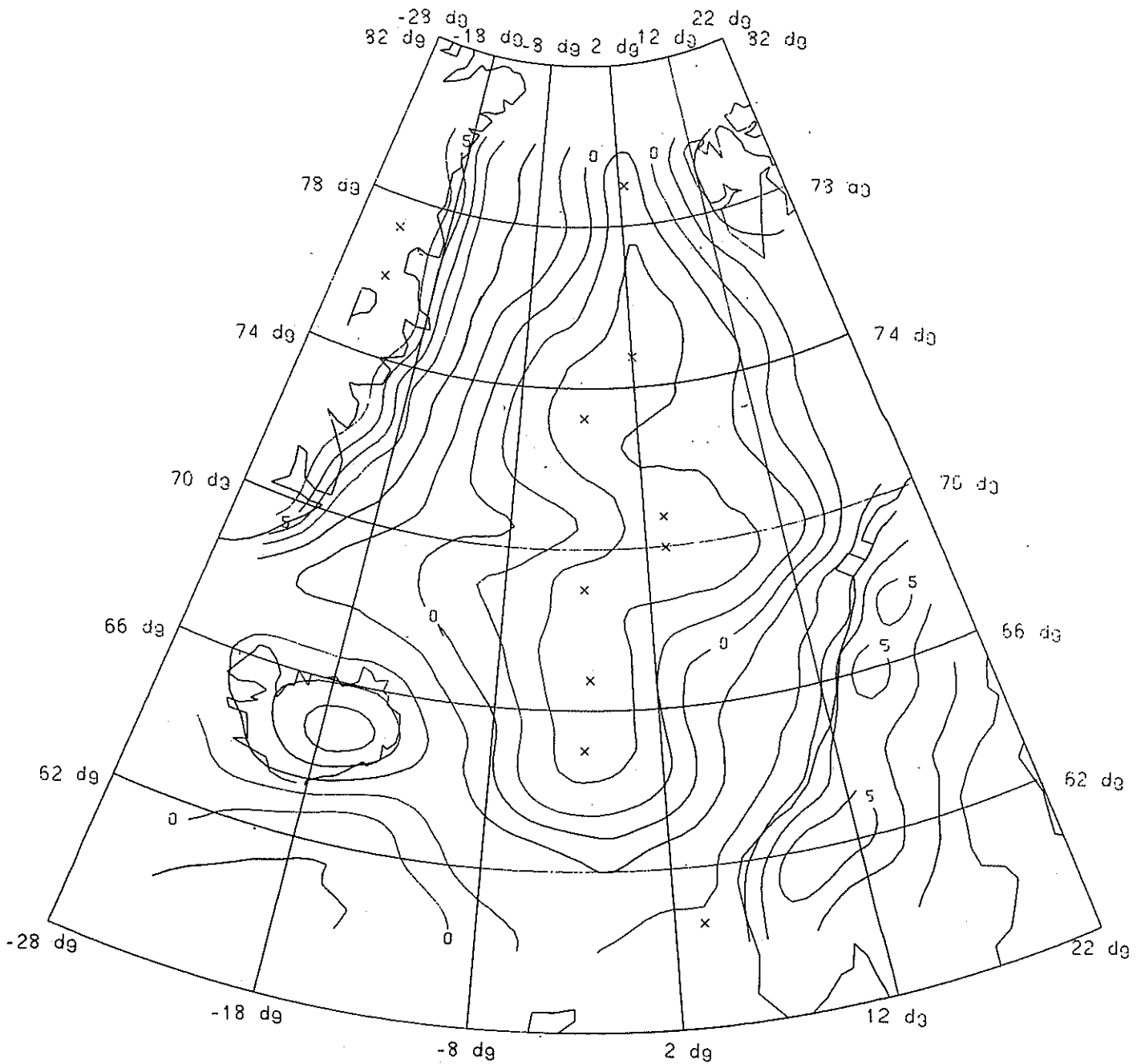


**Fig. 9**  
 Insostatic geoid effects, calculated from 1° X 2° mean heights. Airy-Heiskanen isostatic model used with T = 32 km. Contour interval 1 m.

Forsberg and Madsen (1981), Tscherning (1981), Tscherning and Forsberg (1978), Arabelos (1980) or Wenzel (1980). We are in practice able to make many improvements, all depending on the available data and the computer facilities. We have carried out a local improvement of the geoid (based on Rapp-180) in the area bounded by latitude 66.5° in north, and longitude 7.5° west and 16.5° east. We used point gravity values spaced approximately 10' apart, where

available. For the computation we used least-squares collocation as described in Tscherning (1978). The covariance function used was

$$\text{cov}(T(P), T(Q)) = \sum_{i=2}^{180} (2i + 1) (3 \times 10^{-19}) \left(\frac{GM}{R}\right)^2 + \sum_{i=181}^{\infty} \frac{300 \text{ mgal}^2/R^2}{(i-1)(i-2)(i+24)} \left(\frac{R_b}{r_{prQ}}\right)^{2i+1} P_i(\cos\psi), \quad (6)$$

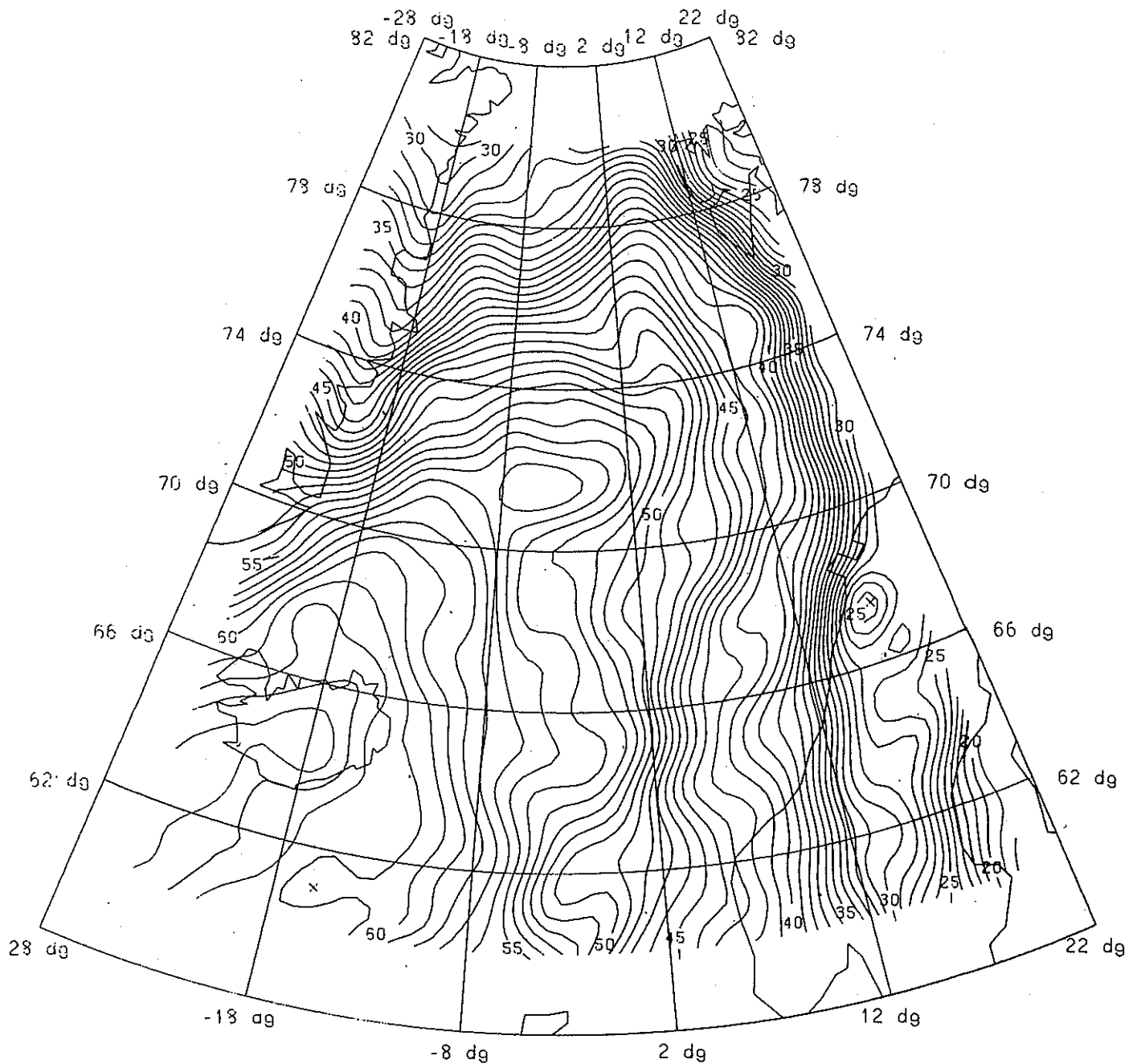


**Fig. 10**  
Isostatically reduced geoid, based on Rapp-180 and the isostatic effects (Figure 9). Contour interval 1 m.

where  $\psi$  is the spherical distance between P and Q. (It was chosen so that it approximated an empirically determined covariance function).

The result is shown in Fig. 6. Note, that the magnitude of the "corrections" to the geoid undulations do not exceed 2.3 m (Fig. 7). The computed geoid undulations agree slightly better with the SEASAT-A data and the discrepancy between a doppler derived geoid undulation and the

computed value decreased from  $-1.8$  m to  $-0.5$  m, see Table I.

### 5. Isostasy and the Medium-Wavelength Geoid

In order to investigate whether a knowledge of the bathymetry and topography could be utilized to strengthen the determination of the geoid we computed isostatic geoid

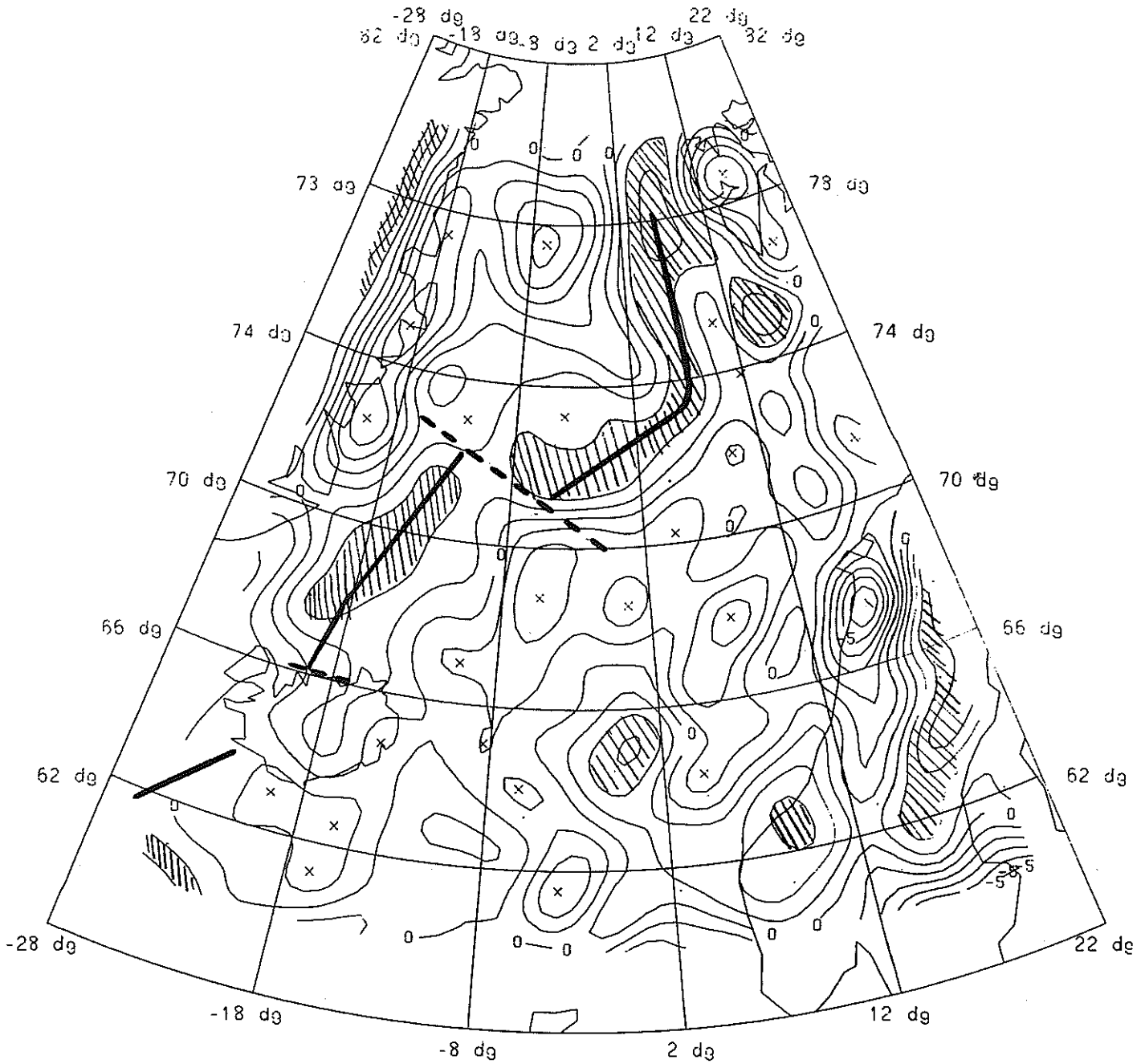


**Fig. 11**  
 Medium-wavelength isostatic geoid. Contour interval 1 m. Areas with residual undulations above 2 m shown hatched. The approximate position of the axis of the mid-atlantic ridge shown as a fat broken curve.

effects according to an Airy-crust of normal thickness  $T = 32$  km, taking all height variations on the Earth into account. The calculation was performed using rectangular prisms for modelling the masses, cf. Forsberg and Tschering (1980). As the most detailed height information  $1^\circ \times 2^\circ$  (roughly  $100 \times 100$  km) mean heights were used. The calculated isostatic geoidal effects are shown in Fig. 9.

When compared to the Rapp-180 geoid (Fig. 1A) it is seen that the effects are relatively small and when the reduced "isostatic" geoid is computed (Fig. 10) practically no smoothing occurs. We thus conclude that the use of height and depth data is unnecessary when working with geoid undulation at wavelengths  $> 100$  km (for local applications this conclusion is not valid, see e.g. Forsberg and Madsen (1980)).

For geophysical purposes the isostatic reduction is very useful, especially for gravity anomalies, as it eliminated the influence of the topography in a consistent way both at sea and on land. When comparing the actual geoid to the isostatic geoid (Figs. 1A and 10) it is seen that some parts of the features of the geoid, e.g. the high over Iceland, can be explained to a large extent as an isostatic phenomena. Most features, however, show no correlation with the topography and thus probably originate from deeper density anomalies in the Earth. To enhance the geoid undulations in the wavelength band from 100 to ca. 500 km we have performed a crude high-pass filtering of the isostatic geoid using a 4th order polynomial trend surface. The resulting "medium-wavelength" geoid is shown in Fig. 11. From the figure it is seen that a geoid high seems to correlate well with the position of the mid-atlantic ridge. At a first look this high seems to be of the wrong sign, as it is generally accepted that the upper mantle material underlying the ridge is of relatively low density. However, a ridge in isostatic equilibrium with extraordinarily deep compensating masses (i.e. the mass deficit in the uppermost mantle) would produce a similar undulation pattern (central high flanked by lows), and this probably explains the axial geoid high.

Up to now most geophysical interpretations of the crust and upper mantle have been based solely on gravity anomalies. However, for many problems involving deep anomalous masses geoid undulations can often be used with advantage compared to mean gravity anomalies, as the undulations by their nature are well defined point quantities, relatively unaffected by the topography and local mass irregularities in the crust. Especially for ocean areas covered by altimeter measurements this is true – and one should not hesitate also to use geoids computed based on gravity data, as we are able to combine all types of gravity field data (e.g. using collocation) in an optimal way for the computation of the geoid.

## 6. Conclusion

In this paper, we have seen that gravity field information of an excellent quality, suitable for geodetic and geophysical purposes is available in the Norwegian-Greenland sea. We have also seen, that we have methods available which permit us to construct local improvements or corrections when necessary.

Computations showed, that the contribution to our knowledge of the geoid from the isostatically compensated topography (of wavelength  $> 1^\circ$ ) is small. However, the contribution must be considered when making geophysical interpretations of the geoid undulations with the purpose of extracting information about the density distribution in the Earth's deeper interior.

## References

- Arabelos, D. (1980): Untersuchungen zur gravimetrischen Geoidbestimmung, dargestellt am Testgebiet Griechenland. Wiss. Arb. d. Fachricht. Vermessungswesen der Universität Hannover, Nr. 98.
- Forsberg, R., F. Madsen (1981): Geoid Prediction in Northern Greenland using Collocation and Digital Terrain Models. *Ann. Geophys.*, Vol. 37, pp. 31–36.
- Forsberg, R., C. C. Tscherning (1981): The Use of Height Data in Gravity Field Approximation by Collocation. *J. Geoph. Res.*, Vol. 86, No. B9, pp. 7843–7854.
- Gerstel, M. (1978): Vergleich von Algorithmen zur Summation von Kugelflächenfunktionen. *Veröffend. der Bayer. Komm. f. d. Int. Erdmessung der Bayer. Akademie der Wissen.*, Heft Nr. 38, pp. 81–88.
- Heiskanen, W., H. Moritz (1967): *Physical Geodesy*. W. H. Freeman and Co., San Francisco.
- Lerch, F., C. Wagner, S. Klosko, R. Belott, R. Laubscher, W. Taylor (1978): Gravity Model Improvement Using GEOS-C Altimetry (GEM 10A and GEM 10B). Paper presented American Geophysical Union Spring Annual Meeting, Miami.
- Lerch, F. J., B. Putney, S. Klosko, C. Wagner (1981): Goddard Earth Models for Oceanographic Applications (GEM 10B and 10C). *Marine Geodesy*, Vol. 5, pp. 145–187.
- Moritz, H. (1980): Geodetic Reference System 1980. *Bulletin Géodésique*, Vol. 54, pp. 395–405.
- Ordnance Survey (1981): Report of Investigations into the Use of Satellite Doppler Positioning to Provide Coordinates on European Datum 1950 in the Area of the North Sea. *Professional Papers (New Series) No. 30*.
- Rapp, R. H. (1977): Determination of Potential Coefficients to Degree 52 from  $5^\circ$  Mean Gravity Anomalies. *Bulletin Géodésique*, Vol. 51, pp. 301–323.
- Rapp, R. H. (1978): A Global  $1^\circ \times 1^\circ$  Anomaly Field Combining Satellite, Geos-3 Altimeter and Terrestrial Data. Dept. of Geodetic Science, Rep. No. 278, The Ohio State University, Columbus, 15 p.
- Rapp, R. H. (1979): Global Anomaly and Undulation Recovery Using Geos-3 Altimeter Data. Dept. of Geodetic Science, Rep. No. 285, The Ohio State University, Columbus, 54 p.
- Rapp, R. H. (1980): A Comparison of Altimeter and Gravimetric Geoids in the Tonga Trench and Indian Ocean Areas. *Bulletin Géodésique*, Vol. 54, pp. 149–163.
- Reigber, C., G. Balmino, B. Moynot (1980): The GRIM 3 Earth Gravity Field Model. Presented at International Symposium "Space Geodesy and its Applications", Cannes, 18–21 Nov.
- Rizos, C. (1979): An efficient computer technique for the evaluation of geopotential from spherical harmonic models. *Austr. J. Geod. Surv.*, No. 31, pp. 161–169.
- Tscherning, C. C. (1976): On the Chain-rule Method for Computing Potential Derivatives. *Manuscripta Geodætica*, Vol. 1, pp. 125–141.
- Tscherning, C. C. (1978): A Users Guide to Geopotential Approximation by Stepwise Collocation on the RC4000-Computer. *Geodætisk Institut, Meddelelse No. 53*, København.
- Tscherning, C. C. (1978): Collocation and Least Squares Methods as a Tool for Handling Gravity Field Dependent Data obtained through Space Research Techniques. *Bulletin Géodésique*, Vol. 52, pp. 199–212.
- Tscherning, C. C. (1981): Comparison of some methods for the detailed representation of the Earth's gravity field. *Rev. Geoph. Space Phys.*, Vol. 19, No. 1, pp. 213–221.
- Tscherning, C. C., R. Forsberg (1978): Prediction of Deflections of the Vertical. *Proceedings of the Second International Symposium on Problems related to the Redefinition of North American Geodetic Networks*. U.S. Dept. of Commerce, NOAA, NOS, Washington, pp. 117–134.
- Tscherning, C. C., R. H. Rapp (1974): Closed Covariance Expressions for Gravity Anomalies, Geoid Undulations and Deflections of the Vertical implied by Anomaly Degree Variance Models. Dept. of Geodetic Science, Rep. No. 208, The Ohio State University, Columbus.
- Wenzel, H.-G. (1980): Recent Results of Geoid Determination by Combination Techniques in the North Sea Test Area. *Veröff. d. D.G.K., Reihe B, Heft Nr. 252*, pp. 95–121, München.